Journal of Hazardous Materials 177 (2010) 12–27

Contents lists available at ScienceDirect

Journal of Hazardous Materials

journal homepage: www.elsevier.com/locate/jhazmat

Review

Quantitative risk assessment of CO_2 transport by pipelines—A review of uncertainties and their impacts

Joris Koornneef[a,*], Mark Spruijt[b], Menso Molag[b], Andrea Ramírez[a], Wim Turkenburg[a], André Faaij[a]

[a] Group Science, Technology and Society, Copernicus Institute for Sustainable Development and Innovation, Utrecht University, 3584 CS Utrecht, The Netherlands
[b] TNO, Environment, Health and Safety – Industrial and External Safety, 3584 CB Utrecht, The Netherlands

ARTICLE INFO

Article history:
Received 15 September 2009
Received in revised form
10 November 2009
Accepted 11 November 2009
Available online 18 November 2009

Keywords:
Quantitative risk assessment
Carbon capture and storage
Carbon dioxide pipelines
CO_2 transport
Uncertainty analysis

ABSTRACT

A systematic assessment, based on an extensive literature review, of the impact of gaps and uncertainties on the results of quantitative risk assessments (QRAs) for CO_2 pipelines is presented. Sources of uncertainties that have been assessed are: failure rates, pipeline pressure, temperature, section length, diameter, orifice size, type and direction of release, meteorological conditions, jet diameter, vapour mass fraction in the release and the dose–effect relationship for CO_2. A sensitivity analysis with these parameters is performed using release, dispersion and impact models. The results show that the knowledge gaps and uncertainties have a large effect on the accuracy of the assessed risks of CO_2 pipelines. In this study it is found that the individual risk contour can vary between 0 and 204 m from the pipeline depending on assumptions made. In existing studies this range is found to be between <1 m and 7.2 km. Mitigating the relevant risks is part of current practice, making them controllable. It is concluded that QRA for CO_2 pipelines can be improved by validation of release and dispersion models for high-pressure CO_2 releases, definition and adoption of a universal dose–effect relationship and development of a good practice guide for QRAs for CO_2 pipelines.

Contents

Abbreviations: QRA, quantitative risk assessment; CCS, carbon capture and storage; EGIG, European Gas Pipeline Incident Data Group; OPS, Office of Pipeline Safety; LPG, liquefied petroleum gas.

* Corresponding author at: Copernicus Institute for Sustainable Development and Innovation, Group Science, Technology and Society, Utrecht University, Willem C. Van Unnikgebouw, Room 925, Heidelberglaan 2, 3584 CS Utrecht, The Netherlands. Tel.: +31 030 253 3544; fax: +31 030 253 7601.
E-mail address: j.m.koornneef@uu.nl (J. Koornneef).

0304-3894/$ – see front matter
doi:10.1016/j.jhazmat.2009.11.068

1. Introduction

Carbon dioxide capture and storage (CCS) is a technological option being developed to mitigate CO_2 emissions from point sources. CCS is comprised of the transport of CO_2 from source to sink. This transport can involve one or a combination of transport media (truck, train, ship or pipeline). Transport by pipeline is considered as the preferred option, especially for large quantities of CO_2 over distances of up to 1000 km [1]. There is already a significant amount of experience with transporting large quantities of CO_2 by pipelines under high pressure, particularly in the United States of America (USA) where over 6000 km of CO_2 pipelines are being operated primarily for Enhanced Oil Recovery (EOR) projects [2,3]. However, the existing CO_2 infrastructure worldwide is very modest compared to the existing hydrocarbon infrastructure.

It should be noted that the experience gained with transporting CO_2 on a large scale in the USA may not directly be applicable to other regions or situations. For instance, most CO_2 pipelines in the USA are situated in remote areas with low population densities. This influences the external safety and precaution measures taken. The deployment of CCS in other regions, e.g. Northwest Europe, will imply that a large network of CO_2 pipelines is needed which will be located in densely populated areas. The special report of the IPCC on CCS has identified the lack of experience with safety issues surrounding the operation of CO_2 pipelines in densely populated areas as a gap in knowledge [1].

Managing external safety comprises the assessment of risks affecting local residents due to the operation of CO_2 pipelines. Assessing these risks can be done quantitatively by estimating the probability and impact of the failure of CO_2 pipelines. Important considerations are the specific properties such as toxicity, corrosiveness and thermo-physical properties. Several quantitative risk assessments (QRAs) for CO_2 pipelines have already been performed [4–14]. A review of these risk assessments allows the identification of uncertainties in risk assessments. This kind of information is at present lacking. Direct comparison of risk assessments is difficult or even impossible as methodologies and other input parameters vary considerably between studies. As a result, the risk of a pipeline failure is assessed with a very large bandwidth. For example, in studies the calculated distance from the pipeline at which the CO_2 concentration exceeds the adopted exposure threshold ranges from <1 m [5] up to 7.2 km [9].

This variation leads to opposing views and controversies around the risks of CO_2 transport. On the one hand, it is suggested that risks of CO_2 transport are known and that CO_2 pipelines do not pose a higher risk than is already tolerated for transporting hydrocarbons or other dangerous substances [6,8]. Other authors also suggest that risks associated with CO_2 transport are well understood [15,16]. On the other hand, it is suggested that there is no significant experience with designing CO_2 pipelines and that CO_2 pipelines near population areas may pose a higher risk than pipelines transporting hydrocarbons [17].

From this preliminary review it can be concluded that there is no consensus on the risks of transporting CO_2 by pipeline. Furthermore, a systematic overview of the impact of methodological choices and selection of input parameters on the results of QRAs for CO_2 pipelines is currently lacking. These two findings form the rationale for this study.

The goal of the study is three-fold: first, to identify (additional) knowledge gaps and uncertainties in QRAs concerning CO_2 pipelines. Second, to assess to what extent those gaps and uncertainties affect the outcome of a QRA for CO_2 pipelines and third, to identify the most critical gaps so that recommendations can be made on R&D priorities to improve QRAs for CO_2 pipelines in the short and medium term.

2. Methodology

In this study, a systematic evaluation of the impact of methodological choices and uncertainties in input parameters on the results of QRAs is presented. This is done by performing a sensitivity analysis for a QRA for a hypothetical pipeline using release, dispersion and impact models in conjunction with a literature review of existing QRAs.

Risk can be defined as the product of the probability and effect of an accidental adverse event. Performing a QRA for CO_2 pipelines first involves the determination of failure scenarios. These failure scenarios have a certain probability attributed to them based on expert judgment or heuristics: in this case experiences with pipeline operations and failures. To estimate the effect, or impact, of a failure scenario, dedicated models are used to calculate the release and dispersion of escaping CO_2. The exposure of local residents to CO_2 is then modelled by estimating the concentration of CO_2 at a certain location after an elapse of time. With a pro-

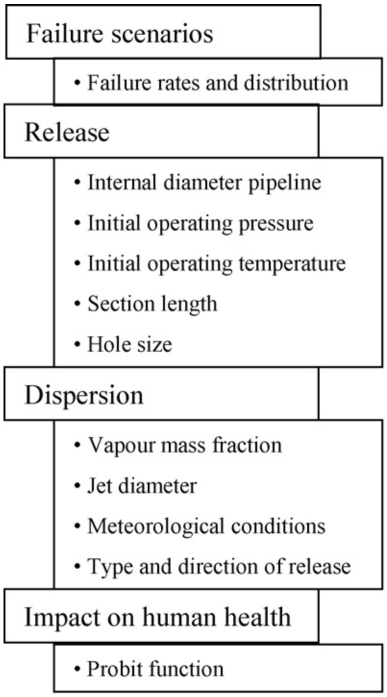

Fig. 1. Overview of important steps to be concluded in a quantitative risk assessment. Per step the methodological choices and input parameters evaluated in this study are shown.

bit function[1] the relationship between exposure to CO_2 and the effect on human mortality rates can be integrated into the calculations. This information allows individual risk contours[2] to be drawn. When the population density surrounding the CO_2 pipeline is known the societal risk can also be determined.

In the section below, existing QRAs for CO_2 pipelines are reviewed and major assumptions in distinctive steps of a QRA for CO_2 pipelines are discussed. These steps are, consecutively, the formulation of the failure scenarios and their probabilities, modelling the release and dispersion of the CO_2 and determination of the impact on human mortality.

In this review we present a selection of parameter values and methodological choices made and their impacts on the results of the QRA (see Fig. 1). For every parameter and methodological choice a default value is assumed. When the value of a parameter is varied to estimate the sensitivity of its outcome, all other parameters are set at their default value.

Our assessment is done using two commercially available software packages developed by TNO: EFFECTS and RISKCURVES [19–21]. A detailed description of the models and the software can be found elsewhere [19].

2.1. Failure scenarios and their probability

Two types of failure scenarios are considered in general when performing a QRA for pipelines, namely a puncture and a full bore rupture [18,22]. In this study we follow this approach. A failure is caused predominantly by third party interference, corrosion, construction or material defects (e.g. welds), ground movement or operator errors [6,23]. In the Netherlands, standard failure rates apply depending on whether the pipeline meets the requirements of the pipeline code (NEN 3650) or whether it is situated in a reserved lane for pipelines [18]. Within these standards the distribution of failure between a full bore rupture and puncture is set to be 0.25:0.75. Other studies use a 50:50 distribution, see [14] or they use a distributed failure profile accounting for a relationship between hole size, pipeline diameter and failure frequency, see [8].

Overall, cumulative failure rates assumed in studies on the risks of CO_2 pipelines ranges from 0.7 to 6.1 per 10,000 km per year (see also Table 1). The fact that failure rates assumed are often based on natural gas pipelines or pipelines in general is a shortcoming. Natural gas pipeline failure rates may not be valid for CO_2 pipelines due to its properties during transport. In addition, failure rates for CO_2 pipelines based on historical accidents cannot be compared straightforwardly with those of natural gas pipelines given the limited cumulative experience with CO_2 pipelines.

Typical properties of CO_2 transport that may justify using different, i.e. higher, failure rates for CO_2 pipelines are the acidity of the CO_2 when dissolved in water and the presence of impurities in the CO_2 stream. Both may lead to corrosion. At least 3 of the 36 incidents between 1994 and 2007 concerning CO_2 pipelines in the USA were caused by corrosion [26]. Minimising water content in the CO_2 flow is therefore important. Experience with pipelines suggests that corrosion rates are very low if the free water content is sufficiently low [26]. Next to free water content other impurities such as SO_x, NO_x, O_2 and H_2S may increase corrosion rates which may lead to higher failure frequencies if not addressed properly [23,26,27]. The effect of impurities in the transported CO_2 on the outcome of the QRA is not taken into account in our study, see Section 4.

In this study three variants are investigated to evaluate the effect of assuming various cumulative failure rates (see Table 2). The effect of these variants on the risk profile of CO_2 pipelines is presented in Section 3.3.1.

2.2. Release

A critical step is the defining of the physical phenomena that take place during the accidental release from a pipeline. These phenomena comprise the dimensions and aspects of the source (area, height, direction), amount, velocity and duration of release, and the thermodynamic state of the substance [18].

The release is substance-specific as thermo-physical properties vary. These properties determine, for instance, the thermodynamic state (pressure, volume, temperature) during the release. In this study the thermo-physical data for CO_2 is taken from [28]. For the solid phase properties we use data from [29]. The release of CO_2 following a puncture or rupture is physically different and is consequently modelled differently.

The release following a full bore rupture is calculated using a model for non-stationary two-phase outflow from a large pipeline in the cases where CO_2 is transported in the liquid phase [30]. This model was originally developed to account for two-phase outflow from an LPG (liquefied petroleum gas) pipeline but could, according to [19], be generalized for other substances by using appropriate physical properties. The model is expected to result in conservative estimates according to [19]. Its validity for CO_2 releases is, however, unknown.

In cases where the CO_2 is transported in the gas phase, a model for a non-stationary outflow from a gas pipeline is used. The outflow model is coupled with a spray-release model and a dense gas dispersion model based on the SLAB model [21]. The spray-release

---

[1] The probit function has the form: $Pr = a + b \times \ln(C^n t)$. Pr is a representation of the response fraction, e.g. percentage of people fataly injured. In this equation a, b and n are substance specific constants describing the lethality related to a dose of a toxic substance, explosion or heat, C is the concentration (in kg/m^3) and t is the exposure time (in s) [18].

[2] An individual risk contour depicts the probability per year on a topographical map that an unprotected ever-present person dies at a certain distance from the pipeline due to the release of the CO_2. Important contours in the Netherlands are the 1×10^{-6} and 1×10^{-8} contours that reflect, respectively, the safety distance and the assessment distance.

Table 1
Failure frequencies used for CO_2 pipelines.

Cumulative failure rate (sum of all failure scenarios) ($\times 10^{-4}$ km^{-1} year^{-1})	Failure scenarios and distribution between rupture and puncture	Source	Comments
6.1	Rupture: 25% Puncture (20 mm): 75%	[11,12,18]	Underground pipeline meeting the requirements of Dutch pipeline code NEN 3650.
0.7	Rupture: 10% Puncture (20 mm): 90%	[18]	Underground pipeline situated in a reserved lane.
20	Rupture: 25% Puncture (20 mm): 75%	[18]	Remaining underground pipeline in the Netherlands (non NEN 3650 or pipelines situated in reserved lane).
2.1 (42 in.); 2.5 (36 in.); 3.1 (24 in.)	Rupture: 10%; large puncture (100 mm): 10%; small puncture (25 mm): 30%; pinhole (5 mm): 50%	[6,8]	Based on data adapted from EGIG[a].
3.4	Full bore rupture: (25%); large puncture (100 mm): 6%; medium puncture (30 mm): 8%; small puncture (7 mm): 41%	[9]	–
1.55	Rupture: 50% Puncture: 50%	[14,24]	Failure rates used for Souris CO_2 pipeline supplying Weyburn oil field.
1.8	Rupture: 33% Puncture (80 mm $\times$ 30 mm): 67%	[5,25]	Based on data from OPS[b] (1994–2006).
3.2	–	[23]	Failure rates based on data from OPS[b] (1990–2001) assuming 2800 km of CO_2 pipelines.
4.1	–	Own calculations	Failure rates based on data from OPS[b] (1994–2007) assuming 6300 km of CO_2 pipelines.

[a] European Gas Pipeline Incident Data Group.
[b] Office of Pipeline Safety [25].

model models the jet properties and possible fallout of solid CO_2 after the expansion of the pressurized content. The SLAB model distinguishes between horizontal jet, vertical jet and instantaneous releases. Sublimation of possible fallout CO_2 is modelled with an evaporating pool model for gases denser than air.

The puncture failure scenario is modelled using the TPDIS[3] model [31] to estimate the two-phase discharge from the pipeline. Further, the linkage of subsequent models (spray-release and dense gas dispersion models) is done in a similar way to that of the full rupture failure scenario.

Important outcomes of the release model(s) are fed into the linked dispersion model. These outcomes are the release rate (kg/s), duration of release, exit temperature, vapour mass fraction and diameter of the 'jet'. The effect of varying assumptions for the inputs for the release models on the maximum and representative release rate[4] and the vapour mass fraction of the release is assessed and presented in Section 3.1. Selected release model inputs are presented in Table 3.

2.3. Dispersion

Typically, a dispersing heavy gas will form a cloud that moves close to the ground, its progress being influenced heavily by local topography and obstructions. The dispersion of a heavy gas is different from gases that are lighter than air, e.g. natural gas. According to Britter [33] and CPR [19] the following reasons can be identified for the difference:

- The substance is typically stored in a liquid phase which represents a very large volume of gas.
- The release is usually transient and can be a mixture of phases.
- The formation of the gas cloud typically involves phase changes.
- Heat and mass transfer with underlying surface are likely to occur.
- The substance encounters gravity-induced spreading.
- The density variations may reduce vertical mixing by stratification of the dispersing cloud.

These characteristics certainly apply to the dispersion of CO_2 as the substance is likely to be transported in a liquid phase. As a consequence, during release, phase transitions are expected to occur which may result in the transfer of heat and mass with the surface, e.g. in the case of dry ice fallout.

The limitation of the dense gas dispersion model and the release models is that they have not been specifically developed for CO_2. Moreover, they have been developed for the gas/liquid phase only and are therefore not equipped to address the solid phase appropriately [19,34].

Table 2
Cumulative failure rates and distribution among ruptures and punctures as assumed in this study for the selected variants. Values highlighted in bold represent the default value.

Parameter	Variants		
Cumulative failure rates (incidents km^{-1} year^{-1})	**6.1×10^{-4}**	0.7×10^{-4}	1.55×10^{-4}
Distribution between type of failure (rupture:puncture)	**0.25:0.75**	0.25:0.75	0.50:0.50

[3] TPDIS is an acronym for Two-Phase DIScharge of liquefied gases through a pipe.
[4] Time varying source terms from release are approximated by one 'constant' representative outflow to make the linkage of outflow and dispersion models possible. This approximation is done by dividing the total mass released into five segments. Each segment has its own duration. The average release rate is then calculated for the second segment, the segment in which the second 20% of the total mass is released. This average release rate is considered the representative flow [18]. A similar approach is adopted in [9].

Table 3
Selected values of the parameters to estimate the influence of each parameter individually on the release of CO_2 from a failing pipeline. Values highlighted in bold represent the default value.

Parameter	Variants				
	1	2	3	4	5
Pipeline internal diameter (mm) (*in.*)	102 (*4*)	203 (*8*)	**406 (*16*)**	610 (*24*)	914 (*36*)
Initial operating pressure (bar)	40[a]	80	**110**	150	200
Initial operating temperature (°C)	**9**	13	17	21	25
Length of isolable section (km)	2	5	10	**20**	50
Hole size (mm)	5	20	50	200	**Full bore rupture**

[a] For the 40 bar variant a different configuration of sub-models is used: the model 'Non-stationary gas release from a long pipeline' replaces the Morrow model. See [32] for more details about the model.

Table 4
Parameters and their values selected to estimate their influence on the dispersion of released CO_2 from a failing pipeline. Values highlighted in bold represent the default value.

Parameter	Variants					
	1	2	3	4	5	6
Vapour mass fraction in release[a] (% mass vapour)	10	20	40	60	80	100
Jet diameter (m)	0.4	**0.63**	0.8	1.2	1.6	2
Meteorological conditions (Pasquill stability classes[b]/wind speed in m/s)	B/5	D/2	D/5	D/9	E/5	**F/2**

Parameter	Variants		
	1	2	3
Type and direction of release	Jet release (**horizontal** and vertical)	Instantaneous release	Sublimating bank[c] (10% fallout and 20% fallout)

[a] The default value for the vapour mass fraction is 70%.
[b] Pasquill atmospheric stability classes: A, very unstable; B, unstable; C, lightly unstable; D, neutral; E, stable; F, very stable.
[c] The sublimating dry ice bank is based upon an evaporating pool model including thermodynamic properties of CO_2 in the solid phase.

Important factors that affect the dispersion of CO_2 that are assessed and discussed in detail in this study are the formation of a crater, weather conditions (atmospheric stability and wind speed), vapour mass fraction or quality, source dimensions, and the type, direction and momentum of the release. The source dimensions are in this case represented by the diameter of the expanded jet. The parameters presented in Table 4 are assessed with the use of the dense gas dispersion model.

2.3.1. Crater formation

If a high-pressure pipeline fails resulting in a large leak or rupture the pressure will drop rapidly, releasing a significant amount of stored energy into its surroundings. In cases where the pipeline is buried, the soil lying above will be ejected into the air causing the formation of a crater[5] [22,36]. The shape and size of such a crater is expected to have an influence on the behaviour of the released matter, i.e. the momentum and direction of the released CO_2 and consequently further dispersion. According to Bartenev et al. [37] the energy potential per unit length of the pipeline, which is a function of the diameter and pressure, is an important factor in pipeline accidents and a decisive factor when determining crater formation. The depth of the pipeline and type of soil are also important parameters that determine the size of the crater together with the angles of the crater wall, see e.g. [36]. These determine the direction of the outflow from the crater and may also influence the momentum of the released CO_2 as the jet impinges on the soil and loses velocity and mass. The modelling of an impinged jet (75% reduction of velocity) is adopted in the approach followed by Turner et al. [8] to model horizontal releases. This may in turn influence the possible formation of a dry ice bank and with it the overall dispersion process [38]. Molag and Raben [12] assumed a crater of 20 m in length by 10 m[6] wide after the failure of a 16.5 bar CO_2 pipeline. No model was used, however, to estimate these dimensions.

In this study no crater formation is assumed as no detailed crater model appears to exist for CO_2 pipelines. The possible implications of this omission are discussed in Section 4.

2.3.2. Vapour mass fraction and jet diameter

Phase transition is an important phenomenon during release and has consequences on the dispersion of CO_2. Phase transition occurs when a pressurized liquidized gas such as CO_2 which is likely to be transported through pipelines suddenly encounters a pressure drop. If the pressure in the pipeline drops, the CO_2 will expand adiabatically which results in a cooling of the pipeline content. When the pressure reaches the saturation line (see Fig. 2), a transition front into a two-phase flow of gas and liquid CO_2 occurs as a consequence of the evaporation of part of the CO_2 (flashing). Flashing ultimately results in the formation of solid CO_2, or 'dry ice', and CO_2 in a gaseous state. The dry ice has a higher density than its surroundings and may fall out onto the ground. Recently conducted CO_2 release and dispersion tests indicate that solid CO_2 sublimes rapidly resulting in no fallout onto the ground [39]. Another test involving the high-pressure (>9.2 MPa) release of CO_2 rich gas from a well resulted in the formation and precipitation of water ice and dry ice [40].

Some uncertainties in flash calculations are highlighted by Calay and Holdo [41] who concluded that the conditions of the flashing jets as a result of the release of liquefied gases are important for the further calculating of the dispersion.

In [5], a sensitivity analysis was performed to study the effect of the vapour mass fraction on the release of the dispersion of the CO_2. The results suggested that a decrease in the vapour mass fraction from 100% to 50% and 1% will lead to significantly higher

[5] An example is the failure of a 30 in. (762 mm) natural gas pipeline operated at 47 bar in New Mexico (USA). This rupture led to the formation of a crater of about 15 m × 35 m (width × length). This pipeline had a soil coverage of about 1.5 m [35].

[6] These dimensions were based on the assumption of the rupture of one pipeline section between two welds (10 m) and a crater formation on each side of the pipeline of 5 meter (2 × 5 m = 10 m).

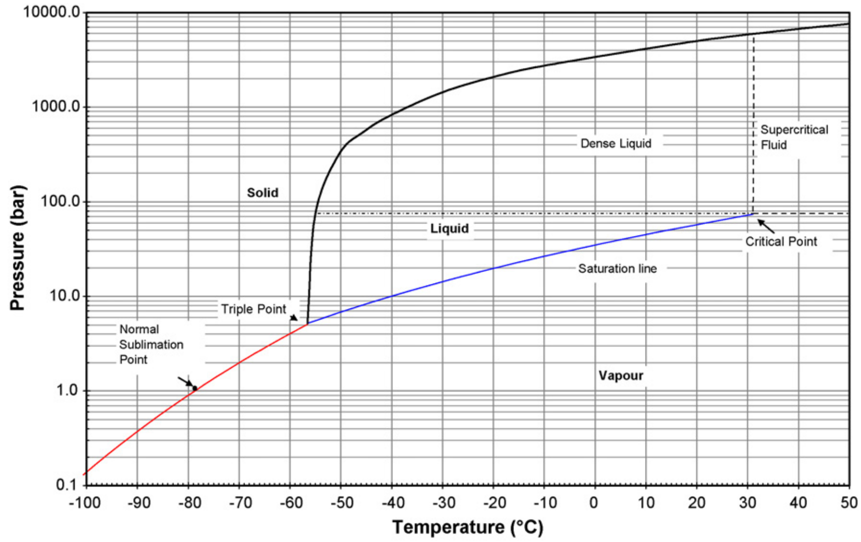

Fig. 2. Temperature–pressure diagram for carbon dioxide.

distances to predefined CO_2 concentration levels between 15,000 and 70,000 ppm.

Gebbeken and Eggers [42] found that the pressure at which flashing first occurs depends mainly on the initial conditions[7] within the vessel containing the CO_2. Also, as the expansion of the CO_2 is assumed to be adiabatic, the vapour mass and dry ice fraction depend on initial conditions, i.e. enthalpy.

In this study the flashed fraction,[8] or vapour mass fraction, is calculated assuming the conservation of enthalpy, momentum and mass [19,43]. Further, it is assumed that CO_2 will expand adiabatically to atmospheric pressure. As a consequence, the temperature of CO_2 after expansion will drop[9] until the sublimation point of CO_2 (−78.5 °C) (see Fig. 2).

Connolly and Cusco [44] suggest that in general the expansion of CO_2 can be considered isenthalpic,[10] though part of the expansion process can be isentropic[11] and thus accurately predicting the thermodynamic states during the expansion brings forth difficulties. This in turn affects the temperature and density, diameter and velocity of the dispersing CO_2 cloud.

The diameter of the jet is another important input for the dispersion model and is one of the parameters varied (see Table 4). It should be noted however that, to maintain the mass balance, increasing the diameter of the jet manually in the model decreases the exit velocity after flashing. The density of the expanded jet is determined by the composition of the vapour–aerosol mixture and will not be affected by changing the diameter in the model.

The characteristics mentioned above (temperature, diameter of the jet and vapour mass fraction) of the expanded release are important inputs for the dispersion model. They are determined in this study with the spray-release model based on representative outcomes (release rate, pressure, temperature and vapour mass fraction at pipeline exit) of the pipeline release model. The model has not, however, been developed and validated for a multi-phase jet containing solid particles. It has therefore been adjusted to cope with this problem provisionally by assuming that the solid phase is a 'liquid' phase with different properties, i.e. the liquid phase is extended and now includes solid phase properties below the triple point. These data on properties are derived from [28,29]. Further, the model includes description of flashing and aerosol formation and evaporation or fallout. Factors that determine whether fallout occurs are the exit velocity of the jet, the size of the aerosols and evaporation rate.

2.3.3. Type and direction of release

The direction and momentum of the released CO_2 has an important impact on the dispersion and consequently on the calculation of risks. This has been shown by Molag and Raben [12,45]. In this study the researchers selected a vertical jet release with momentum as the most likely scenario resulting in a lower figure for the risk. In other risk assessment studies, direction and momentum are often not mentioned (see for instance [4,11]). In [7], the release is handled as an instantaneous puff. In [5], all releases are modelled as horizontal jets as this is considered to be the worst case scenario for dense gases. In [8], both horizontal and vertical releases were modelled. They are also considered as a low momentum release in the case of a horizontal jet as this would collide with the soil and, in so doing, lose momentum. Cameron-Cole [10] modelled both horizontal and vertical releases, and found that the horizontal release led to higher concentrations at ground level. Vendrig et al. [9] assumed a loss of momentum during release (due to the impact on surrounding soil), and a liquid release resulting in the formation of a pool that subsequently evaporates contributing to a vapour cloud. The formation of a liquid pool of CO_2 is however not possible at atmospheric pressure (see Fig. 2). The formation of a dry ice bank as a result of fallout is, however, possible. For a scenario with fallout, Bricard and Friedel [38] envisage lower concentrations further downwind from the source with the trade-off of higher con-

[7] Lower initial temperature leads to a lower pressure at which flashing starts to occur. Flashing also starts earlier compared to higher initial temperatures. A lower initial pressure leads to higher pressures at which flashing starts to occur.

[8] The flash fraction is the amount of CO_2 that has flashed, i.e. the gaseous mass fraction directly after flashing has occurred.

[9] Kruse and Tekiela [7] assumes that adiabatic expansion occurs which leads to a drop of the temperature down to up to the triple point (−56.4 °C). This is however not possible under atmospheric conditions.

[10] Isenthalpic expansion assumes that the enthalpy is equal before and after expansion of the system. No heat is exchanged and no work is extracted from or done on the system. In [5] it is assumed that isenthalpic expansion occurs and it is calculated that after expansion 74% of the released CO_2 is in the vapour phase and 26% in the solid, with initial conditions of 15 MPa and 35 °C.

[11] Isentropic expansion is the adiabatic and thermodynamically reversible expansion of the CO_2. This means that the expanding CO_2 does positive work on its surroundings, i.e. the atmosphere. Heijne and Kaman [13] assumes isentropic expansion to occur resulting in 68% gaseous CO_2 and 32% dry ice after expansion from initial conditions of 31.5 MPa and 105 °C. Assuming isentropic expansion will lead to a lower vapour mass fraction in the flashed release compared to isenthalpic expansion as less available heat in the compressed CO_2 is used for evaporation (due to the drop in enthalpy) [34].

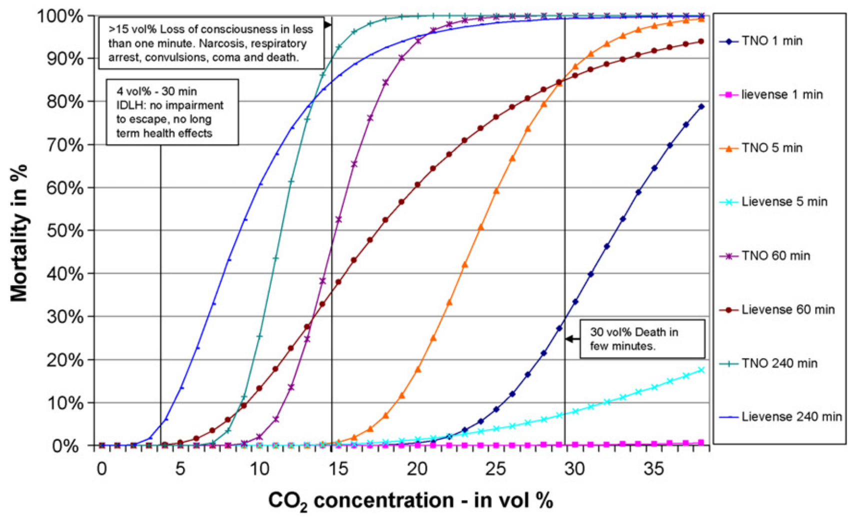

Fig. 3. Comparison of probit functions as defined by Molag and Raben (TNO) [12] and Lievense [11] showing the percentage of mortality in human population as a consequence of various levels and durations of exposure to CO_2. Also other exposure thresholds as presented by Hepple [57] are shown for comparison.

centrations near the source and an increase in the duration of the release.

In this study the type (jet, instantaneous, an evaporating accumulation) and direction (horizontal and vertical) of the release is varied in the dense gas dispersion model (see Table 4). The sublimating dry ice bank is based upon an evaporating pool model including thermodynamic properties of CO_2 in the solid phase. In that variant it is assumed that 10%, respectively 20%, of the release of the default scenario (see Table 3) is falling out and forming a dry ice bank with a surface of 100 m^2. The rate of sublimation is assumed to be equal to the amount added to the bank, which is known, from [46], likely to result in an over-estimation of gaseous CO_2. Furthermore, it is only the contribution of the sublimation of the dry ice bank to a CO_2 cloud that is calculated here. The remaining 90% and 80% of the released CO_2 is not taken into account. This will result in an underestimation of the CO_2 concentration. In the scenario describing an instantaneous release, it is assumed that 20% of the total mass released in the default scenario is released instantly as a puff of CO_2.

2.3.4. Meteorological conditions

According to literature, meteorological conditions have an important influence on the risk of a release of CO_2. Vendrig et al. [9] mention the F2 (Pasquill stability class: F, wind speed: 2 m/s) conditions as the most problematic as these stable atmospheric conditions hinder dispersion and result in increased CO_2 concentrations further downwind. A similar conclusion is drawn by other authors [6,8]. Another study suggests that for vertical release the D stability class is worse than the F stability class due to “the complex interaction of stability class and elevated plumes” [10]. They used the F1 conditions as worst case scenarios for the horizontal cases to mimic minimal dispersion, which would result in the highest maximum concentrations. TetraTech [5] mentions the D5 and F2 classes as worst cases for horizontal releases as the CO_2 concentra-

Table 5
Sets of failure scenarios (puncture and rupture) developed for synthesis and confrontation with scenarios presented in other studies [8,9,11,12].

Set	Parameter						
	Section length (km)	Hole size[a] (mm)	Vapour mass fraction[b] (%)	Jet diameter[c] (m)	Type of release[d]	Failure rate (incidents km^{-1} year^{-1})	Probit function
S1	20	406	70	0.63	*Instantaneous*	6.1×10^{-4}	TNO-probit
S2	20	406	70	0.63	*Instantaneous*	*0.7×10^{-4}*	TNO-probit
S3	20	406	70	0.63	Horizontal	6.1×10^{-4}	TNO-probit
S4	20	406	70	0.63	*Instantaneous*	6.1×10^{-4}	*Lievense-probit*
S5	20	406	70	0.63	*Instantaneous*	*1.55×10^{-4}*	TNO-probit
S6	20	406	*100*	0.63	Horizontal	6.1×10^{-4}	TNO-probit
S7	20	406	*10*	0.63	Horizontal	6.1×10^{-4}	TNO-probit
S8	20	*914*	*72*	*2*	Horizontal	6.1×10^{-4}	TNO-probit
S9	20	406	70	*0.5*	Horizontal	6.1×10^{-4}	TNO-probit
S10	20	406	70	*2*	Horizontal	6.1×10^{-4}	TNO-probit
S11	20	406	70	0.63	*Vertical*	6.1×10^{-4}	TNO-probit
S12	20	406	70	0.63	*Sublimating bank 10%*	6.1×10^{-4}	TNO-probit
S13	20	406	70	0.63	*Sublimating bank 20%*	6.1×10^{-4}	TNO-probit
S14	*50*	406	70	0.63	Horizontal	6.1×10^{-4}	TNO-probit

Note that assumptions deviating from the default scenario are highlighted italic. The release conditions in the puncture scenario are assumed to be the same for all sets, the only exception being the failure rate (S2 and S5). Note that for all sets an equal distribution among the following weather classes is assumed: B3, D1.5, D5, D9, E5 and F1.5. Non varied assumptions are: pipeline roughness: 0.045 mm; wind speed (at 10 m height): 2 m/s; ambient temperature: 9 °C; concentration averaging time: 600 s; height of release and receptor: 1 m; ambient relative humidity: 83%; wind direction is equal to direction of release; roughness length description (roughness of terrain): 0.25 m (high crops; scattered large objects, upwind distance < 15 m, height of obstacles < 20 m); discharge coefficient full rupture: 1; discharge coefficient puncture: 0.62.

[a] For all puncture scenarios a hole size of 20 mm is assumed.
[b] For all puncture scenarios a vapour mass fraction of 21% is assumed.
[c] For all puncture scenarios a jet diameter of 21 cm is assumed.
[d] For all puncture scenarios a vertical release is assumed.

tions remain elevated at distances further away from the source. Results of the study by Vendrig et al. [9] indicate F2 as being more detrimental as compared to D5. However, they assumed a type of release (evaporating pool) that is significantly different from the other studies.

Mazzoldi et al. [47] considered the D5 and F2 weather classes for an approximately horizontal release in their study. They calculated the maximum downwind distances to the concentration limits (15,000 and 100,000 ppm) while varying weather class and release velocity (0 m/s vs. 49 m/s). The results show that the F2 weather class is the worst case situation for the release without velocity and the D5 is the worst case for the release with velocity. Overall, the maximum distance from the pipeline to the 100,000 ppm contour (i.e. 1290 m) is found for the release without velocity under F2 weather conditions.

To estimate the impact of meteorological conditions on the dispersion in this study, six variants are composed by varying wind speed and atmospheric stability classes (see Table 4).

2.3.5. Effect on human health

After determining the release and dispersion of the CO_2 it is necessary to estimate the expected impact of elevated CO_2 concentrations on human health. To determine health effects not only the CO_2 concentration is important but also the duration of the exposure. CO_2 can cause serious adverse health effects at certain concentration levels and duration of exposure. Lethal asphyxiation is, for instance, reported from 110,000 ppm and loss of consciousness at 100,000 ppm (for 3–5 min) and 300,000 ppm (for less than 1 min). Halpern et al. [48] mentions >17% vol. (170,000 ppm) as the concentration that may cause lethal poisoning.

CO_2 displaces oxygen resulting in asphyxiation. However, also under normal oxygen concentrations high CO_2 concentrations are harmful. CO_2 is thus not only an asphyxiant but also directly toxic at high concentrations [49]. An increased level of CO_2 lowers blood pH and changes the composition of chemicals in the blood.

The effects on human health of exposure to certain concentrations of CO_2 are well documented and comprehensive reviews have been written, see e.g. [50–54]. However, these reviews indicate some knowledge gaps in CO_2, which are:

- Acute and chronic exposure to the more vulnerable and sensitive populations still has to be evaluated as current knowledge is based on tests with healthy subjects [52,55].
- Threshold concentrations shown by most literature studies are relatively old. Results from more recent studies, showing lower acceptable concentrations, still need to be validated [50].

Furthermore, Turner et al. [8] as well as Hundseid and Ingebrigtsen [56] highlight the absence of the publication of the probit function in international literature. Up to now pipeline risk assessments have shown a divergence in threshold values of several orders of magnitude for the exposure to CO_2 assumed to cause an effect (see Appendix A). This variance indicates that there is no single international standard for the application of an exposure threshold for CO_2.

Two different probit functions for CO_2 have been proposed and used for CO_2 in QRAs in the Netherlands. In Fig. 3 the main difference between the two proposed probit functions in relation with exposure thresholds mentioned in literature is presented. The probit function proposed by Lievense [11] shows the probability of mortality to be higher for longer during exposure compared to the probit function proposed by TNO in [12]. Due to the shape of the probit function of TNO, mortality rates are higher for higher concentrations. The probit function of Lievense is thus more dependent on the duration of exposure while the function of TNO is more dependent on the concentration. Both probit functions are, however, not based on extensive experimental work and are therefore not formally adopted. The publication of a new probit function for CO_2 based on experimental work with rats for the use in QRAs in the Netherlands is expected to be available in 2009.

The effect of applying either of the two proposed probit functions is assessed and presented in Section 3.3.6.

2.3.6. Synthesis

The end result of the QRA is (in this study) the maximum distance to the individual risk contour. In this section the synthesis step is described. This step is performed to analyze the effect of multiple parameters on the end result of the full QRA. In total 14 sets of failure scenarios have been developed. Each set consists of two failure scenarios: one for a full rupture and one for a puncture. Every set can be compared to at least one other set where one parameter is different, ceteris paribus (see Table 5). The values for the parameters in these scenarios have been chosen to represent the ranges presented in Tables 2–4 and those found in literature. The results are expected to resemble a range that reflects optimistic and conservative approaches. The results of the synthesis step will be discussed by comparing sets of failure scenarios that have been formulated in this study (indicated by an 'S' in Table 5).

3. Results

In this section the results of varying the parameters, or variants, as presented in Tables 3 and 4 are discussed subdivided into a section presenting the effects on the release followed by a section discussing the effects on dispersion. In Section 3.3 the results of the synthesis step are presented. The results are finalized with presenting risk-mitigation options for CO_2 pipelines.

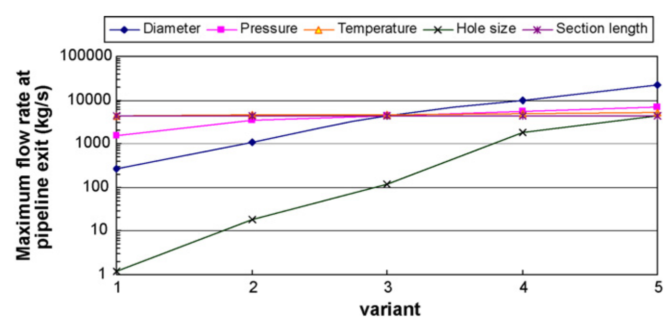

Fig. 4. Variance in maximum flow rate at pipeline exit with varying diameter, pressure, temperature, section length and hole size.

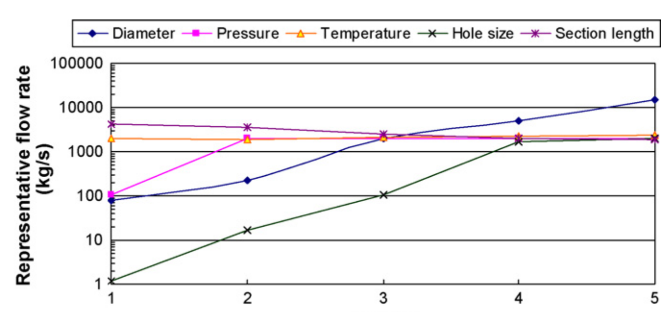

Fig. 5. Variance in representative flow rate at pipeline exit with varying diameter, pressure, temperature, section length and hole size.

3.1. Release

In Figs. 4 and 5 the effect of varying the parameters diameter, pressure, temperature, section length and hole size on the maximum and representative exit flow rate is shown. Note that variants are presented in Table 3 and that for every variant holds that all parameter values are at their default value except for the parameter being varied. All variants are modelled with the use of the Morrow model (two-sided outflow) except variants 1–4 of the parameter 'hole size' and variant 1 of the parameter 'pressure'. These are derived with the TPDIS model and the model for non-stationary gas release through a long pipeline, respectively.

The results in Figs. 4 and 5 show that the parameters with largest influence on the maximum and representative flow rate are the diameter of the pipeline and the size of the orifice, while temperature has the smallest influence. This is further discussed per parameter.

3.1.1. Initial pressure

In the case of a rupture the conditions in the pipeline change significantly over time. The outflow is, at first, about equal to the maximum outflow but as pressure and temperature decrease, the outflow diminishes over time. When increasing the initial pressure the outflow is initially higher but diminishes steeply with time. When initial pressures are above the saturation pressure, it seems that flow rates stabilize at 2 tonnes/s for all cases studied approximately 300 until 600 s after rupture.

3.1.2. Initial temperature

Varying initial temperature has relatively little influence on the maximum and representative flow rate, as shown in Figs. 4 and 5. The maximum mass flow rate is, respectively, 4.3 tonnes/s and 5.2 tonnes/s for the 9 °C and 25 °C variant. The main difference between the variants is that the level at which the flow rate remains is almost constant after a certain amount of time. This level is lower for the variants with higher initial temperatures. Further, stabilization of the flow rate occurs later.

3.1.3. Pipeline diameter

The sensitivity of the results to the diameter of the pipeline is large, as varying the diameter results in a change in the maximum and representative flow rate of over one order of magnitude. Also, when increasing the diameter of the ruptured pipeline choked flow[12] conditions are sustained for a longer time period (approximately 200 s for 914 mm, versus 14 s for 102 mm). Thus higher exit pressures are expected together with higher flow rates for longer time periods. On the other hand, the duration of a release increases with a decrease of the diameter.

3.1.4. Hole size

Figs. 4 and 5 clearly show that increasing the hole size in the case of a puncture will increase the maximum and representative flow rate with several orders of magnitude. As the release from a hole is expected to stay almost constant over time, the maximum flow rate and representative flow rate do not differ by much.

3.1.5. Distance between block valves

The distance at which block valves divide the pipeline in a number of sections has no influence on the maximum flow rate. It does however have an influence on the duration of the release, on the total amount of CO_2 that is released and on the representative release rate. The representative release rate is significantly higher as the section lengths decrease. This can clearly be seen by comparing Figs. 4 and 5. However, this is due to the methodology[4] adopted to determine the representative release rate and is not a physical effect. That is, the second 20% of the total mass is released at higher rates when shortening distances between block valves. This results in a higher representative release rate.

3.1.6. Vapour mass fraction at orifice exit

The influence of systematically varying initial pressure and temperature on the flash fraction at the orifice exit has resulted in the following findings. For pressures above the critical pressure, varying the pressure has no influence on the initial (24%) and maximum flashed (44%) fraction. It has an effect on how the flashed fraction evolves over time. In general, the higher the initial pressure the sooner the maximum vapour mass fraction in the release is reached. The flash fraction drops after reaching the maximum and settles at 29% for all variants. For pressures below the critical pressure the CO_2 is in the gaseous phase during transport and as a consequence no flashing occurs. The vapour mass fraction is thus 100%.

The initial and maximum vapour mass fraction increase with an increase in the initial temperature to respectively 34% and 60% for the highest temperature variant (25 °C). Furthermore, the higher the temperature the longer it takes before the maximum vapour mass fraction is reached. The vapour mass fraction drops after reaching the maximum and is between 29% and 57% for respectively variant 1 and 5 at the orifice exit at the end of the release.

Increasing the diameter of the pipeline will result in a delay for the maximum vapour mass fraction in the release to be reached. Changes in the section length have very little effect on the evolvement of the vapour fraction.

3.1.7. Flash fraction after full expansion

In general, increasing the initial temperature in the pipeline leads to higher vapour fractions at the pipeline orifice. After full expansion of the CO_2 release to atmospheric pressure the temperature of the jet drops to the sublimation temperature for all cases. The vapour fraction after expansion increases with initial vapour fraction and varies between 70% and 79% for the 9 °C and 25 °C variants, respectively. This agrees with the fractions suggested in [5]. The diameter of the expanded jet increases with the vapour mass fraction and varies between 0.6 and 0.8 m for respectively variant 1 and 5. No fallout of solid CO_2 is expected to occur for all variants.

Increasing initial operating pressures when above the saturation pressure does not have a large influence on the initial vapour mass fraction and consequently on the flashed fraction after full expansion (70% for all cases). Consequently, the pressure also has no or very small influence on the diameter of the jet. This is found to be 0.7 m for all variants except variant 1. In this variant the initial pipeline pressure is below the saturation pressure, i.e. no flashing occurs and the spray-release model could not be applied. Also when varying the operating pressure no fallout of solid CO_2 is expected for all cases.

For the puncture scenarios the calculations show somewhat different results. In the TPDIS model it is assumed that the initial release is a pure liquid release, i.e. a vapour mass fraction of 0% [20]. The linked spray-release model calculates the vapour mass fraction in the expanded jet to be about equal for the puncture cases between 21% and 22%. No fallout is expected to occur in the puncture cases.

[12] Choked flow directly relates to the speed of sound in the gas and is the maximum velocity of the exiting CO_2 if the pressure in the pipeline exceeds a substance dependent pressure criterion, i.e. for CO_2 this criterion is 1.9 times atmospheric pressure.

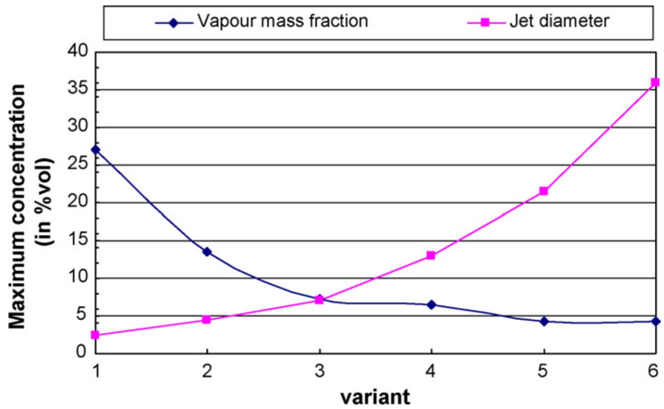

Fig. 6. Effect of changing vapour mass fraction in the release and jet diameter on the maximum concentration calculated with the dense gas dispersion model assuming a horizontal jet.

3.2. Dispersion

3.2.1. Vapour mass fraction

In our study the vapour mass fraction has been varied between 10% and 100%, assuming no fallout of solid CO_2 (see Table 4). Note that variants are presented in Table 4 and that for every variant holds that all parameter values are at their default value except for the parameter being varied. The results in Fig. 6 show that a lower vapour mass fraction in the release will lead to higher maximum concentration in the vicinity of the source. The figure does not show the distance to this maximum concentration. This distance ranges between 71 and 93 m downwind from the source for the 10% case and 100% case, respectively. Furthermore, the vapour mass fraction is expected to influence the shape of the released CO_2 cloud. In general, the lower the vapour fraction the wider the CO_2 cloud and the further the cloud is propagated into a downwind direction. This holds at least for the assessment height of 1 m assumed in our study. This can be explained by the effect of gravity as the density of the cloud increases with increasing solid mass fraction.

3.2.2. Diameter of expanded jet

The diameter of the expanded jet is mainly dependent on the area of the orifice, the density and velocity of the CO_2, before and after flashing. Changes in the diameter of the expanded jet will lead to comparable results as when varying the vapour mass fraction. Namely, increasing the jet diameter or decreasing the velocity after flashing will result in a higher maximum CO_2 concentration (see Fig. 6). Furthermore, wider CO_2 clouds are expected with the maximum concentrations to be found closer to the source.

3.2.3. Type and direction of the release

The results in Table 6 indicate that the variants assuming a sublimating dry ice bank and instantaneous release result in the highest concentration near the source, as in both cases the release occurs without momentum. The opposite is seen for variants with a vertical or horizontal release, where the highest concentration at receptor level is anticipated relatively further away from the source. Another result of the dispersing CO_2 from the sublimating dry ice banks is that elevated CO_2 concentrations (up to 6% vol.) are also expected up to approximately 100 m upwind.

The maximum distance to the lower threshold is the highest for the instantaneous release while in this variant only 20% of the total mass of that in the jet variant is released. The same holds for the sublimating bank variant that also releases 20% of the default variant. This results in greater distances to the 2.7% vol. threshold for this variant (573 m) than found for the jet releases (194–512 m).

For the vertical release a higher maximum concentration is calculated compared to the horizontal release. This maximum is reached further away from the source compared to the other types and direction of releases. In contrast to the other variants, the instantaneous variant starts with a constant high concentration and then follows an exponential decrease. For this variant, higher concentrations compared to the other variants are estimated up to approximately 0.8 km downwind from the source.

It should be noted that the dispersion model shows imperfect results for the instantaneous release variant as it calculates a volume percentage of CO_2 higher than 100%. This is probably the result of a technical or model structure error used to convert units of concentration, i.e. from kg/m^3 to ppm. A refinement of the model is in this respect needed.

3.2.4. Meteorological conditions

Fig. 7 shows that, under F2 conditions, elevated CO_2 concentrations as a result of a horizontal release can be expected further downwind compared to the other weather classes. However, concentrations near the source show to be the highest under D9 (31% vol.) and B5 (12% vol.) conditions for the horizontal release. For the vertical release the results show that significantly elevated concentrations are only expected under stable and neutral atmospheric conditions (classes F2 and D2). Under F2 conditions the concentrations are the highest with a maximum of 7% vol. at a distance of 151 m from the pipeline. For the vertical release, only the F2 variant results in a concentration higher than the 2.7% vol. threshold.

When comparing the types of releases the results show that for all weather classes the horizontal release results in higher concentrations except under F2 conditions. With respect to all the assumptions made in this study the results indicate that the more unstable weather classes result in maximum CO_2 concentrations nearer to the source compared to the more stable classes. Under stable weather classes, elevated concentrations can be expected further away from the source.

When comparing the results for the vertical with the horizontal jet release, the difference in calculated concentration as a function of distance is apparent (see Fig. 7). This clearly indicates that the

Table 6
Results of dispersion calculations varying type and direction of release.

Parameter	Jet release		Instantaneous release	Sublimating bank	
	Horizontal	Vertical		10% fallout	20% fallout
Flow rate (kg/s)	1943	1943	–	194	389
Flow duration (s)	1156	1156	–	1156	1156
Total mass released (kg)	2.25×10^6	2.25×10^6	4.5×10^5	2.25×10^5	4.5×10^5
Maximum concentration (Yd = 0, Zd = 1) (% vol.)	5	7	104	6	6
At distance downwind (m)	105	151	0–67	36	21
Maximum distance to 2.7% vol. (50,000 mg/m^3)[a] (m)	194	512	800	385	573
Maximum distance to 5.5% vol. (100,000 mg/m^3)[b] (m)	–	227	524	125	161

[a] This is the alerting exposure limit: irreversible effects may occur when exposure duration is longer than 1 h [58].
[b] This is the life threatening exposure limit: fatality or life threatening injuries may occur when exposure duration is longer than 1 h [58].

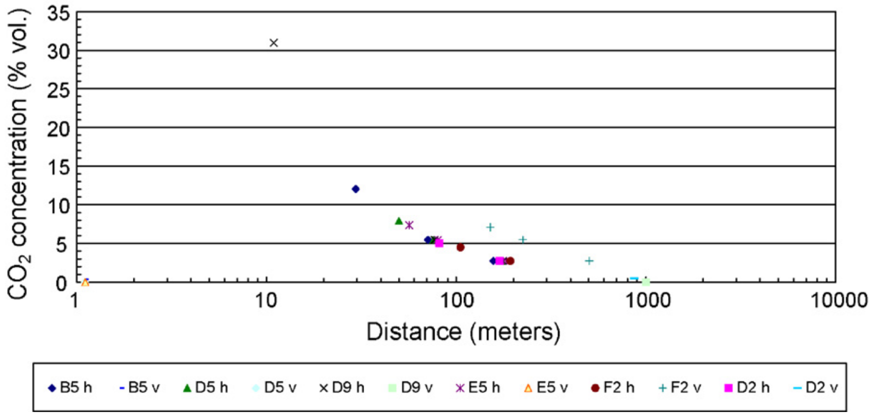

Fig. 7. Effect of meteorological assumptions on distance to maximum and threshold (50,000 mg/m^3 and 100,000 mg/m^3, respectively 2.7 and 5.5% vol.) concentrations for horizontal jet (h) and vertical jet (v). Note that the values calculated for 'E5 v', 'B5 v' and 'D5 v' are not in line with the other results and are likely the result of a model error.

result of the QRA is not only dependent on the type of release but also on the weather class.

3.3. *Synthesis*

Results of the 14 sets of scenarios presented in Table 5 are presented in Table 7 and are compared to results of previously published QRAs for CO_2 pipelines (indicated by 'Ext.').

3.3.1. *Probability of failure*

The results show that none of the puncture scenarios yielded a contribution to the risk of the set of scenarios presented in Table 7. The contribution of punctures, which are expected to be more probable than full ruptures, to the risk of CO_2 pipelines is thus expected to be limited. The effect of varying failure rates and its distribution between puncture and full rupture on the final result of the QRA can be seen in Table 7 by comparing S1, S2 and S5.

Table 7
Results of the sets of failure scenarios formulated in this study (see Table 5) and in previous risk assessments (indicated by 'Ext' followed by a number).

	Maximum distance to risk contour in meters					
	1×10^{-4} [a]	1×10^{-5} [a]	1×10^{-6} [a]	1×10^{-7} [a]	1×10^{-8} [a]	1×10^{-9} [a]
Set of failure scenarios in this study						
S1	–	154	204	235	240	244
S2	–	–	126	190	228	241
S3	–	–	–	–	–	–
S4	–	–	–	91	114	118
S5	–	131	193	229	240	243
S6	–	–	–	–	–	–
S7	–	–	–	116	153	179
S8	–	–	–	–	–	–
S9	–	–	–	–	–	–
S10	–	–	5	97	140	168
S11	–	–	–	–	–	–
S12	–	–	23	50	65	75
S13	–	–	53	86	110	125
S14	–	–	–	–	18	28
Existing studies						
Ext. 1[b]	–	40	1200	–	–	–
Ext. 2[c]	–	70	2700	–	–	–
Ext. 3[d]	–	70	1490	–	–	–
Ext. 4[e]	–	170	3400	–	–	–
Ext. 5[f]	–	–	3.5	11.5	22.5	
Ext. 6[g]	–		21	–		–
Ext. 7[h]	–	–	90	–	–	–
Ext. 8[i]	98	1733	1903	2070	–	–
Ext. 9[j]	160	1866	2441	3000	–	–
Existing regulations						
High-pressure natural gas pipelines[k]	–	–	60	–	180	–

[a] Risk contours (probability of fatality per year).
[b] Onshore pipeline, 30 in. (0.76 m) diameter, 25 °C, 100 bar, 15,000 ppm endpoint [9].
[c] Onshore pipeline, 30 in. (0.76 m) diameter, 25 °C, 100 bar, 2000 ppm endpoint [9].
[d] Offshore pipeline, 40 in. (1.02 m) diameter, 25 °C, 200 bar, 15,000 ppm endpoint [9].
[e] Offshore pipeline, 40 in. (1.02 m) diameter, 25 °C, 200 bar, 2000 ppm endpoint [9].
[f] The values shown are the maximum values reported based on: NEN 3650 failure rates and a probit function by Lievense [11].
[g] Pipeline pressure of 16.5 bar, 26 in. (0.66 m) diameter, NEN 3650 failure rates and a probit function by TNO [12].
[h] Pipeline pressure of 40 bar, 26 in. (0.66 m) diameter, NEN 3650 failure rates and a probit function by TNO [12].
[i] Pipeline diameter of 42 in. (1.07 m), EGIG failure rates, horizontal release, 70,000 ppm endpoint [8].
[j] Pipeline diameter of 24 in. (0.61 m), EGIG failure rates, horizontal release, 70,000 ppm endpoint [8].
[k] Regulated distances for natural gas pipelines in Netherlands for pipelines with a pressure of 80–110 bar and a diameter of 48 in. (1.22 m) [59].

For the S2 (set with the lowest failure rates) the 1×10^{-6} individual risk contour lies at a maximum distance of 126 m from the pipeline contrary to the 204 m found for S1 with the highest failure rates. Furthermore, the 1×10^{-6} risk contour for S1, S2 and S5 stretches out further away from the CO_2 pipeline than is being currently regulated in the Netherlands [59] for high-pressure natural gas pipelines, i.e. 60 m. It should be mentioned that such safety distances have not yet been defined for CO_2 pipelines in the Netherlands.

3.3.2. Type and direction of the release

The effect of varying the type of release on the risk profile can be seen in Table 7 by comparing S1, S3 and S11, respectively the instantaneous, horizontal and vertical release. The 1×10^{-8} risk contour lies at 240 m for S1 and is not present for S3 and S11. In the rupture scenarios of S12 and S13 it is assumed that a part of the release of the rupture scenario of S3 is expected to fall out. The results show that a 10% fallout results in a 1×10^{-8} risk contour at 65 m from the pipeline. For the 20% variant this distance is 110 m and the 1×10^{-6} risk contour lies then at 53 m. When compared to S3 it is prominent that the dry ice banks, which result in a release rate significantly smaller than for S3, result in a higher risk. An explanation is that for the sublimating dry ice banks, as well as for the instantaneous type of release, maximum concentrations are reached close to the source. In our study both types of release are assumed to be without momentum, i.e. wind speed is the main driver of dispersion which could explain the result. The opposite is seen for the releases with momentum where maximum concentrations are anticipated relatively further away from the source (i.e. further than 100 m). Altogether this indicates that varying the type of release has significant impact on the risk profile of the CO_2 pipeline. Since valid arguments can be made for each type of release, this aspect should be carefully dealt with in future QRAs.

3.3.3. Pipeline diameter

Comparing S3 and S8 presents the effect of the pipeline diameter on the risk profile. For both sets the 1×10^{-9} risk contour lies directly on top of the pipeline, indicating a distance of 0 m. A higher risk for S8 would be expected as this set includes a rupture scenario in which a larger quantity of CO_2 is released. However, the methodology applied in this study to use the representative flow rate (see Section 3.1) weakens the effect of varying the initial diameter of the pipeline. No conclusion can however be drawn based on our results.

3.3.4. Diameter of expanded jet

Increasing the diameter of the expanded jet (and with it decreasing the velocity) will result in higher CO_2 concentrations nearer to the source and a wider CO_2 cloud. The results show that the rupture scenario in S3 with a jet diameter of 0.63 m yields no 1×10^{-8} risk contour versus a distance of 140 m found to that in S10 with a jet diameter of 2 m. The risk of S9 (diameter of 0.5 m) is also too low to be shown in Table 7.

3.3.5. Vapour mass fraction

The effect of varying the vapour fraction on the final risk profile is large, as can be seen by comparing S3, S6 and S7. The greatest distance – 153 m for the 1×10^{-8} risk contour – is found for the S7 with the lowest vapour fraction in the release (10%). The risks calculated for S3 and S6 with vapour fractions of respectively 70% and 100% are too low to be shown. This indicates that there is a significant difference in risks as an effect of the vapour fraction.

3.3.6. Dose–effect relationship

Set S1 with a probit function suggested by TNO and S4 with a probit function suggested by Lievense [11] show a difference in the risk profile (see Table 7). S4 has no 1×10^{-6} risk contour. This compared to the 204 m distance for S1 indicates a higher risk for S1. Furthermore, the 1×10^{-8} risk contour lies 126 m further away for S1 (151 m) compared to S4 (240 m).

The effect of assuming a threshold for CO_2 concentrations instead of a probit function can also be significant, see also Section 2.3.5. This can be seen by reviewing the results of previous QRAs. In current literature a wide range (2000–100,000 ppm) of thresholds, including non-lethal, are used to construct the risk profiles. Using the lower end of these thresholds can result in the most extreme case in a 1×10^{-6} risk contour at 3.4 km from the CO_2 pipeline (Ext. 4 in Table 7).

In general, scenarios which include concentration thresholds (with or without a specification of the duration of the exposure) instead of probit functions result in a higher risk. Although other factors cannot be ruled out, this is expected to be primarily the result of using conservative concentration thresholds for which an adverse impact is assumed on human health. This can be clearly seen by comparing Ext. 1–4. The scenarios with the 2000 ppm thresholds (Ext. 2 and Ext. 4) have their 1×10^{-6} risk contour over a factor of two further away compared to the scenarios with the 15,000 ppm threshold (Ext. 1 and Ext. 3).

3.3.7. Decrease distance between block valves

Decreasing the distance between block valves should have a positive effect on the risk profile as it decreases the duration of the release and total amount of released CO_2, and consequently duration and level of exposure. The results show for S14 (50 km between valves) that the 1×10^{-8} risk contour is at a distance of 18 m whereas for S3 (20 km between valves) this distance is zero. Thus, according to our study, installing block valves at shorter distances does indeed has a risk-mitigating effect.

Hooper et al. [6] however suggest that installing block valves would have limited risk-mitigating effects as isolation would not occur in time to limit the initial flow rates that have the most adverse impact on the CO_2 concentration. A block valve may also be a potential component of failure and will add to cost when installed at shorter distances. Moreover, higher quality pipeline materials may be required near the block valves [17].

3.4. Risk-mitigation measures

Risk-mitigation measures are typically aimed at: (1) reducing the exposure to a failure mechanism; (2) increasing the resistance to a failure mechanism; (3) mitigating the effect of a failure, and (4) limiting the impact of a failure on the environment. The first two are focussed on reducing the probability of failure and the latter two on mitigation or remediation of the consequences of a failure. The mitigation of risk is possible by implementing available technical, administrative and socio-psychological measures that may address any of these goals. In Table 8 a non-exhaustive list is presented of risk-mitigation measures appearing in literature.

The results of our study suggest that risk-mitigation should be focused on reducing the probability of large releases and on reducing the impact of these releases as they have the most adverse consequences in the case of failure.

These measures presented in this overview will have economic consequences that have to be evaluated. The necessity of applying extensive mitigation measures will depend on specific situations (e.g. high population density, large diameter pipeline) and should also be evaluated as such. Therefore, clearly an optimum has to be

Table 8
Selection of available mitigation measures for CO_2 pipelines based mainly on [12,32,60–62].

Risk-mitigation measure	Quantitative or qualitative description of risk reduction factor compared to pipeline without the measure
Increase soil coverage[a]	~1 m extra soil coverage yields factor 10 reduction in failure rate caused by third party interference.
Coverage with protective material and physical barriers	
Warning tapes above pipeline	Factor 1.67 reduction in failure rate.
Concrete barrier above pipeline	Factor 5 reduction in failure rate.
Warning tapes and concrete barrier combined	Factor 30 reduction in failure rate.
Fencing	Third party interference hardly possible.
Dike above pipeline (>1 m height)	Factor 10 reduction in failure rate.
Barrier at ground level (sheet piling, concrete fence stake marking)	Factor 8 reduction in failure rate.
Management agreements in which:	
Level 1: Far reaching limitations to use of the area are in effect;	Factor 100 reduction in failure rate.
Level 2: Soil disrupting activities are not allowed;	Factor 10 reduction in failure rate.
Level 3: Moderate limitations of use of the area are in effect (e.g. soil disruption is allowed to a certain depth)	Factor 1.6 reduction in failure rate.
Increase pipeline wall thickness	Reduce possibility of third party damage; increase resistance to corrosion.
Corrosion protection	Reduce failure rate caused by corrosion.
Coating (inner and outer); cathodic protection; pipeline material selection; inhibitor injection; cleaning (e.g. sweeping of liquid accumulations); CO_2 purity requirements	
Increase survey interval	Early detection of CO_2 release.
Install block valves	Reduce duration of CO_2 release and total amount of CO_2 released, see Section 3.3.7.
Route selection	Reduction of the possibility for human exposure to increase CO_2 concentrations.
Avoid terrain with topographical depressions	
Avoid densely populated areas	
Addition of tracers to CO_2 (odour and/or colour)	Early detection of CO_2 release.
Educating	Reduce the impact by educating surrounding communities on specific properties of CO_2, its release and possible remediation actions following a failure of the pipeline.

[a] Approximated by $y = 1.01e^{2.39x}$ where x is the extra soil coverage (m) and y is the reduction factor [32].

found between risk (decreasing failure rate, shorter duration and less mass released) and economy [23] also taking into account the risk perception issues [63].

4. Discussion

Overall, the results show that the most conservative distance of the 1×10^{-6} risk contour to the CO_2 pipeline in our study is calculated to be at 204 m. This distance is in the same order of magnitude as the currently regulated distances for high-pressure natural gas pipelines. For comparison, a liquefied petrol gas filling station with a throughput of 1000 m^3 per year is set in Dutch regulations to have a 1×10^{-6} contour of up to 120 m. For refrigerating installations or heat pumps containing between 8 and 10 tonnes of ammonia this contour is set at a maximum of 110 m [64]. The conservative distance for CO_2 pipelines calculated in this study is thus in the same order of magnitude as the legally set distances for installations containing hazardous materials or transport infrastructure for natural gas.

Whether the risks of CO_2 pipelines are formally or legally acceptable will strongly depend on local conditions like population density and other risk-bearing activities. Whether the risks are socially acceptable will depend on public attitude. This is determined more by psychological factors than merely a quantified representation of the risk presented in the form of a individual risk contour (see also [63]).

Quantifying the risks of CO_2 pipelines accurately is at present difficult. The way to mitigate these risks is, however, part of existing knowledge and existing risk-mitigation measures can be applied on CO_2 pipelines.

Reviewing the results, the outcome of the QRA can be influenced by regulating pipeline design and operation parameters by, for example, assessing their failure rate, section length, pipeline diameter, operating pressure and operating temperature. Remaining parameters can be influenced by standardizing the QRA methodology which includes both methodological choices as the structure and technical implementation of the QRA model.

For the most part, uncertainty in the outcome of a QRA for CO_2 pipelines stems from the methodological choices made in the assessment. These are choices about dose–effect relationships and type (direction and momentum) of release. In this study, variation in these choices leads to a variance in the distance to the 10^{-6} risk contour between 0 and 204 m and thus dominates the outcome. Standardization of these choices would simplify the comparison of QRAs. Also in practice the variance calculated for the outcome of the QRA can mean the difference between the formal acceptance and rejection of a CO_2 pipeline design or route.

Other methodological choices like the linkage of sub-models for release and dispersion are embedded in the structure and technical implementation of the applied QRA model. A comparison between other QRA (sub) models versus the EFFECTS and RISKCURVES software used in this study would yield insight into uncertainty that stems from the model structure and technical implementation of the model in computer software [65]. The structure and technical implementation of the model can be improved by performing field tests for the validation of the QRA models for CO_2 pipelines. Improving scientific rigor would reduce the degrees of freedom for the methodological choices to be made by the party performing the QRA and with it reduce variance in the outcome of QRAs.

Other issues, knowledge gaps or uncertainties in the assessment of risks of CO_2 pipelines are:

- Smaller pipelines are reported to show relatively higher failure rates compared to pipelines with a large diameter [6]. No differentiation is assumed in this study for different pipeline sizes; thus a simplification is applied here.
- The effect of a crater formation on the release of CO_2 is only qualitatively described in this paper. It may affect the momentum and angle of the CO_2 release and as such the precipitation and dispersion of the CO_2. However, it is not expected that applying a crater model would result in exceeding the risks calculated in our study for the most conservative scenario.
- It is not discussed here whether a release of supercritical CO_2 from a pipeline differs significantly from dense liquid release [42]. In this study only the risks of CO_2 pipelines operating below supercritical conditions are studied.
- The impact of impurities on the release is not studied here. Next to engineering problems, impurities might also result in impacts on human safety as some of these substances are highly toxic (predominantly H_2S and CO). Turner et al. [8] considered the presence of impurities in the CO_2 stream in the risk assessment. The impurities, including H_2S (0.2%) and CO (0.7%), showed to have a small effect on the risk profile that was dominated by the toxicity of CO_2 whereas the result of another study showed a significantly higher distance to the exposure threshold for H_2S (up to 1180 m) than for the CO_2 content (up to 210 m) of the released material [14]. Another study also indicated a larger distance (nearly 6 times) to the exposure threshold for H_2S (50 ppm) compared to that of CO_2 (70,000 ppm) [5]. Impurities thus may dominate the risk profile.
- This brings forth additional uncertainties regarding the assessment of the release and subsequent dispersion of the CO_2 and the impurities. It may also influence the final impact on human health depending on the concentration and toxicity of the impurity.
- In our study the effect of crosswinds on the dispersion of the CO_2 cloud is absent. Mazzoldi et al. [66] indicate that this will influence the dispersion and thus exposure to CO_2.
- Clogging of holes due to dry ice and/or hydrates formation in the pipeline may influence the release rate at the exit of the pipeline. This is not accounted for in this study.
- Rapid cooling of the CO_2 may induce thermal stress in the pipeline and in materials of adjacent installations and/or exposed pipelines. Also the explosive expansion and possible formation of projectiles may inflict damage to properties (adjacent pipelines) and humans in the direct vicinity [67]. This is of particular interest when CO_2 pipelines are planned to join routes of, for instance, natural gas pipelines or other pipelines transporting hazardous substances. The failure of a CO_2 pipeline may then induce failure of the adjacent pipeline(s). Estimating the potential domino effect of a failing CO_2 pipeline is therefore recommended. By such a study minimum distances to be applied between parallel pipelines can be determined.
- Overpressure as a result of the sudden expansion may also cause direct harm to humans, even fatality, in the direct circumference of the pipeline [67]. Molag and Raben [12] report 100% fatality[13] (0.3 bar overpressure) within 3 m for a pipeline transporting CO_2 at 16.5 bar. Such effects have not been taken into account in our study.

Clearly, these limitations mentioned above indicate that the uncertainty surrounding the risk assessment of CO_2 pipelines has not been mapped completely. An assessment of the impact of those uncertainties, preferably quantitatively, on the result of a QRA is therefore recommended.

[13] They also report 2.5% lethality within 5 m.

5. Conclusion

In this study the review of existing QRAs has allowed the identification and discussion of knowledge gaps and uncertainties in QRAs for CO_2 pipelines. A systematic assessment of the impact of a number of these gaps and uncertainties on the (intermediate) results of a QRA for CO_2 pipelines has been presented. The results show that when performing a QRA that takes into account the probability of a failure, release and dispersion of CO_2 and the impact on health, knowledge gaps and uncertainties can have a large impact on the accuracy of calculated risks of CO_2 pipelines.

It is argued why it is not certain whether failure rates for natural gas pipelines can be used for CO_2 pipelines. Rates that have been used in other QRAs and in this study are between 0.7×10^{-4} and 6.1×10^{-4} km^{-1} year^{-1}. As a result the distance to the 1×10^{-6} risk contour may vary between 126 and 204 m.

Modeling the release of CO_2 from a failing pipeline also brings forth uncertainties. Variance in the maximum release rate of a pipeline failure, which ranges between 0.001 and 22 tonnes/s, is mostly influenced by, in order of importance: the size of the orifice, the diameter of the pipeline (in the case of a full bore rupture), operating pressure, operating temperature and section length.

Furthermore, there is a lack of knowledge about the vapour and dry ice fraction in the release. This parameter has a large influence on the dispersion and consequently on the risk profile of CO_2 releases: a distance varying between 0 and 153 m between the pipeline and 1×10^{-8} risk contour is calculated. A recommendation that follows is that release and dispersion field tests should be set up to measure the vapour fraction and the impact of dry ice formation on the dispersion of the release.

A methodological choice that affects the QRA's outcome to a large extent is the direction and momentum of release. Results for the 1×10^{-6} risk contour vary between 0 and 204 m as a consequence. Currently, there is no consensus on the type of release that is characteristic for a CO_2 release from a failing pipeline. The results indicate that when varying the type of release, the calculated distances from the pipeline to the 1×10^{-6} risk contour may be larger than currently regulated for high-pressure natural gas pipelines.

In addition, uncertainty is caused by the absence of a dose–effect relationship as well as internationally standardized exposure thresholds for CO_2 for use in QRAs. This results in a large divergence of results in QRAs for CO_2 pipelines. In this study the risk contour is found at a distance between 0 and 204 m when varying the probit function. The results of earlier risk assessments varied between <1 m and 7.2 km assuming different exposure thresholds.

Results also indicate that the risks of CO_2 pipeline punctures are expected to be significantly lower than that of ruptures. Mitigation of risks should be focused on reducing the probability and consequences of large releases and less on reducing the probability and consequences of small scale leaks. Options for mitigating these risks are available but will add cost to the pipeline infrastructure.

Besides the knowledge gaps and uncertainties investigated in this study, other uncertainties and knowledge gaps have been identified that deserve further attention. In this study priorities to improve QRAs for CO_2 pipelines on the short and medium term have been formulated. First, validation of release and dispersion models is necessary for high-pressure CO_2 by performing experiments and field tests. Such tests should include CO_2 streams with impurities to analyze the effects of release and dispersion. Second, the definition and adoption of a universal dose–effect relationship (preferably a probit function) for CO_2 is desirable. In the mean time, it is necessary to define uniform concentration and exposure thresholds for CO_2 to be used in QRAs. Third, when there is a significant uncertainty related to a methodological choice or value for an input parameter in the QRA, the worst case outcome of that specific choice or input should be reported following the precautionary principle. Finally, it is recommended to develop a good practice guide for QRAs for CO_2 pipelines.

Acknowledgements

This research is part of the CATO programme. CATO is the Dutch national research programme on CO_2 Capture and Storage. CATO is financially supported by the Dutch Ministry of Economic Affairs under the BSIK programme. The authors would like to acknowledge this financial support and the people who commented on earlier versions of this article: Koos Ham (TNO) and Peter Hochs (TNO). Finally, we would like to thank the reviewers for their valuable comments.

Appendix A. Exposure thresholds assumed in other QRAs for CO_2 pipelines

Source	Exposure threshold(s) (ppm)	Exposure as function of concentration and time?	Comments
[9]	2000 15,000	No	Thresholds are not considered to be lethality thresholds.
[8]	70,000 (several min)	It is unclear whether duration of exposure is included in the calculations	No explicit duration mentioned. Threshold is "conservatively attributed to causing fatality".
[14]	40,000 – 30 min (IDLH)[a] 100,000 – 1 min (LC_{lo})[b]	It is unclear whether duration of exposure is included in the calculations	Concentrations thresholds are used instead of exposure thresholds.
[5]	20,000 – 8 h 40,000 – 8 h 30,000 – 15 min 40,000 – 15 min	It is unclear whether duration of exposure is included in all the calculations	For puncture and rupture different concentration thresholds are used.
[7]	50,000 – 1 min	Yes	Exposure threshold explicitly mentioned as 50.000 ppm for 60 s.
[4]	100,000	No	Assumed to be fatal concentration.
[11]	54,647 (100,000 mg/m^3) – 60 min	Probit function[c]: $Pr = -0.91 + 1 \times \ln(C^2 t)$	This exposure is assumed to result in 1% lethality. This exposure threshold is used to derive the probit function.
[12,45]		Probit function[c]: $Pr = 4.45 + 1 \times \ln(C^{5.2} t)$	Probit function is based on the average of the following assumptions: 4 h exposure to 10% vol. results in 1% lethality; 5 min exposure to 20% vol. results in 99% lethality.
[10]	5000 (10 min) TWA[d] 30,000 (STEL)[e]	It is unclear whether duration of exposure is included in the calculations	

[a] Immediately dangerous to life or health.
[b] Lethal concentration lower limit.
[c] C in kg/m^3; t in s.
[d] Time weighted averages.
[e] Short term exposure limit.

References

[1] IPCC, IPCC Special Report on Carbon Dioxide Capture and Storage, Cambridge University Press, Cambridge, United Kingdom/New York, NY, USA, 2005, p. 442.
[2] J.T. Kelliher, Testimony of the Honorable Joseph T. Kelliher Chairman of the Federal Energy Regulatory Commission, Committee on Energy and Natural Resources of United States Senate, 2008.
[3] J.O. Kadnar, Experience in CO_2 transportation via pipeline, in: CCS Web Conference on CO_2 Transport, Health and Safety Issues, International Energy Agency, Paris, 2008.
[4] D. Golomb, Transport systems for ocean disposal of CO_2 and their environmental effects, Energy Convers. Manage. 38 (Suppl. (1)) (1997) S279–S286.
[5] TetraTech, Final Risk Assessment Report for the FutureGen Project Environmental Impact Statement, Lafayette, CA, USA, 2007.
[6] B. Hooper, L. Murray, C. Gibson-Poole, Latrobe Valley CO_2 Storage Assessment, CO2CRC, Melbourne, Australia, 2005.
[7] H. Kruse, M. Tekiela, Calculating the consequences of a CO_2-pipeline rupture, Energy Convers. Manage. 37 (6–8) (1996) 1013–1018.
[8] R. Turner, N. Hardy, B. Hooper, Quantifying the risks to the public associated with a CO_2 sequestration pipeline: a methodology & case study, in: Greenhouse Gas Control Technologies 8, Trondheim, 2006.
[9] M. Vendrig, J. Spouge, A. Bird, J. Daycock, O. Johnsen, Risk Analysis of the Geological Sequestration of Carbon Dioxide, Department of Trade and Industry, London, UK, 2003.
[10] Cameron-Cole, Air dispersion modelling of well blowout and pipeline rupture scenarios. Salt Creek field, in: RETEC, EDM International Inc., Centennial Archaeology Inc., Cedar Creek Associates Inc., BKS Environmental Associates Inc. (Eds.), Environmental Assessment Howell Petroleum Phase III/IV CO_2 Enhanced Oil Recovery Project: Salt Creek Oil Field, U.S. Department of the Interior, Bureau of Land Management, Casper Field Office, 2005.
[11] Lievense, OCAP CO2 v.o.f. CO_2 Greengas project - Risico analyse NPM-leiding document 042282 rev. 3, Raadgevend Ingenieursbureau Lievense B.V., Breda, 2005.
[12] M. Molag, I.M.E. Raben, Externe veiligheid onderzoek CO_2 buisleiding bij Zoetermeer, TNO, Apeldoorn, 2006, p. 46.
[13] M.A.M. Heijne, F.J.H. Kaman, Veiligheidsanalyse Ondergrondse Opslag van CO_2 in Barendrecht - Appendix 6, in: Haskoning (Ed.), MER Ondergrondse opslag van CO_2 in Barendrecht, Tebodin, The Hague, Netherlands, 2008.
[14] NEB, Reasons for Decision in the Matter of Souris Valley Pipeline Limited, National Energy Board, Calgary, Canada, 1998.
[15] J.J. Heinrich, H.J. Herzog, D.M. Reiner, Environmental assessment of geologic storage of CO_2, MIT LFEE Report, 2004.
[16] K. Damen, A. Faaij, W. Turkenburg, Health, safety and environmental risks of underground CO_2 storage—overview of mechanisms and current knowledge, Clim. Change 74 (1) (2006) 289–318.
[17] J. Barrie, K. Brown, P.R. Hatcher, H.U. Schellhase, Carbon dioxide pipelines: a preliminary review of design and risk, in: Greenhouse Gas Control Technologies 7, Vancouver, Canada, 2004.
[18] CPR, Guidelines for Quantitative Risk Assessment—The 'Purple Book', Committee for the Prevention of Disasters (CPR), VROM, RIVM, The Hague, Netherlands, 1999.
[19] CPR, 'Yellow Book' Methods for the Calculation of Physical Effects—Due to Releases of Hazardous Materials (Liquids and Gases), Committee for the Prevention of Disasters (CPR), VROM, TNO, The Hague, 2005.
[20] TNO, TNO Safety Software EFFECTS Version 7 User and Reference Manual, TNO Built Environment & Geosciences, Department of Industrial and External Safety, Utrecht, the Netherlands, 2007.
[21] D.L. Ermak, User's Manual for SLAB: An Atmospheric Dispersion Model for Denser-than Air Releases, Physics Department, Atmospheric and Geophysical Sciences Division, University of California, Lawrence Livermore National Laboratory, Livermore, 1990.
[22] R.J. Harris, M.R. Acton, Development and implementation of risk assessment methods for natural gas pipelines, in: CHINA GAS 2001 International Conference with Special Focus on Gas Safety, Chongqing, China, 2001.
[23] J. Gale, J. Davison, Transmission of CO_2—safety and economic considerations, Energy 29 (9–10) (2004) 1319–1328.

[24] D.V. Dorling, Analysis of Reportable Incidents for Natural Gas Transmission and Gathering Lines 1970–1984, American Gas Association, Battelle Memorial Institute, 1990.
[25] PHMSA, Hazardous liquid accident data, Last updated: 06/13/2008, Pipeline and Hazardous Materials Safety Administration, Office of Pipeline Safety, available at: http://ops.dot.gov/stats/IA98.htm, 2008.
[26] E. de Visser, C. Hendriks, M. Barrio, M.J. Mølnvik, G. de Koeijer, S. Liljemark, Y. Le Gallo, Dynamis CO_2 quality recommendations, Int. J. Greenhouse Gas Control 2 (4) (2008) 478–484.
[27] A. Oosterkamp, J. Ramsen, P.N. Seevam, J. Race, M. Downie, Pipeline transport of CO_2 with impurities—a state of the art review, 2007.
[28] DIPPR, DIPPR 801 Database v21.13, Design Institute for Physical Properties, 2007.
[29] M. Azreg-Aïnou, Low-temperature data for carbon dioxide, Monatsh. Chem. 136 (2005) 2017–2027.
[30] T.B. Morrow, R.L. Bass, J.A. Lock, A LPG pipeline break flow model, J. Energy Res. Technol. 105 (1983) 379–387.
[31] J. Kukkonen, Modelling Source Terms for the Atmospheric Dispersion of Hazardous Substances, Finnish Society of Sciences and Letters, Helsinki, 1990, 111 pp. + app.
[32] RIVM, Achtergronden bij de vervanging van zoneringafstanden hoge druk aardgastransportleidingen van de N.V. Nederlandse Gasunie, Rijksinstituut voor Volksgezondheid en Milieu (RIVM), 2008.
[33] R.E. Britter, Atmospheric dispersion of dense gases, Annu. Rev. Fluid Mech. 21 (1) (1989) 317–344.
[34] DNV, Flashing Liquid Jets and Two-phase Dispersion—A Review, Det Norske Veritas, London, 2002.
[35] NTSB, Pipeline Accident Report. Natural Gas Pipeline Rupture and Fire Near Carlsbad, New Mexico August 19, 2000, National Transportation Safety Board, Washington, 2003.
[36] H.N. Duckworth, R. Eiber, Assessment of pipeline integrity of Kinder–Morgan conversion of the Rancho pipeline, Austin, TX, 2004.
[37] A.M. Bartenev, B.E. Gelfand, G.M. Makhviladze, J.P. Roberts, Statistical analysis of accidents on the Middle Asia-Centre gas pipelines, J. Hazard. Mater. 46 (1) (1996) 57–69.
[38] P. Bricard, L. Friedel, Two-phase jet dispersion, J. Hazard. Mater. 59 (2–3) (1998) 287–310.
[39] H.W.M. Witlox, M. Harper, A. Oke, Modelling and Validation of Discharge and Atmospheric Dispersion for Carbon Dioxide Releases, DNV Software, London/College Station, TX, 2008.
[40] J.Q. Xu, G. Weir, L. Paterson, I. Black, S. Sharma, A case study of a carbon dioxide well test, APPEA J. Part 1 (2007) 237–248.
[41] R.K. Calay, A.E. Holdo, Modelling the dispersion of flashing jets using CFD, J. Hazard. Mater. 154 (1–3) (2008) 1198–1209.
[42] B. Gebbeken, R. Eggers, Blowdown of carbon dioxide from initially supercritical conditions, J. Loss Prev. Process Ind. 9 (4) (1996) 285–293.
[43] H. Witlox, M. Harper, P. Bowen, V. Cleary, Flashing liquid jets and two-phase droplet dispersion. II. Comparison and validation of droplet size and rainout formulations, J. Hazard. Mater. 142 (3) (2007) 797–809.
[44] S. Connolly, L. Cusco, Hazards from high pressure carbon dioxide releases during carbon dioxide sequestration processes, in: International Symposium on Loss Prevention and Safety Promotion in the Process Industries, Edinburgh, 2007.
[45] M. Molag, Actualisatie Externe veiligheid onderzoek CO_2 buisleiding bij Zoetermeer, TNO, Utrecht, 2008, p. 17.
[46] A. Mazzoldi, T. Hill, J.J. Colls, CO_2 transportation for carbon capture and storage: sublimation of carbon dioxide from a dry ice bank, Int. J. Greenhouse Gas Control 2 (2) (2008) 210–218.
[47] A. Mazzoldi, T. Hill, J. Colls, A consideration of the jet-mixing effect when modelling CO_2 emissions from high pressure CO_2 transportation facilities, in: 9th International Conference on Greenhouse Gas Control Technologies (GHGT-9), Washington, USA, Elsevier – Energy Procedia, 2008.
[48] P. Halpern, Y. Raskin, P. Sorkine, A. Oganezov, Exposure to extremely high concentrations of carbon dioxide: a clinical description of a mass casualty incident, Ann. Emerg. Med. 43 (2) (2004) 196–199.
[49] C.-C. Hsieh, C.-L. Shih, C.-C. Fang, W.-J. Chen, C.-C. Lee, Carbon dioxide asphyxiation caused by special-effect dry ice in an election campaign, Am. J. Emerg. Med. 23 (4) (2005) 567.
[50] National Research Council, Carbon dioxide, in: Board on Environmental Studies and Toxicology (Ed.), Emergency and Continuous Exposure Guidance Levels for Selected Submarine Contaminants, National Academy Press, Washington, DC, 2004, pp. 37–53 (Chapter 3).
[51] National Research Council, Carbon dioxide, in: Commission on Life Sciences (Ed.), Spacecraft Maximum Allowable Concentrations for Selected Airborne Contaminants, vol. 2, National Academy Press, Washington, DC, 1996, pp. 105–188 (Chapter B3).
[52] S.A. Rice, Health Effects of CO_2, EPRI, 2004.
[53] S.M. Benson, R. Hepple, J. Apps, C.F. Tsang, M. Lippmann, Lessons Learned from Natural and Industrial Analogues for Storage of Carbon Dioxide in Deep Geological Formations, Earth Sciences Division, E.O. Lawrence Berkeley National Laboratory, Berkeley, 2002, p. 135.
[54] K.E. Schaefer, Effects of increased ambient CO_2 levels on human and animal health, Cell. Mol. Life Sci. (CMLS) 38 (10) (1982) 1163–1168.
[55] S. Holloway, J.M. Pearce, V.L. Hards, T. Ohsumi, J. Gale, Natural emissions of CO_2 from the geosphere and their bearing on the geological storage of carbon dioxide, Energy 32 (7) (2007) 1194–1201.
[56] H. Hundseid, K.O. Ingebrigtsen, Human Resistance Against Thermal Effects, Explosion Effects, Toxic Effects and Obscuration of Vision, DNV Technica, Scandpower, 2001.
[57] R.P. Hepple, Human health and ecological risks of carbon dioxide, in: S.M. Benson (Ed.), The CO_2 Capture and Storage Project (CCP) for Carbon Dioxide Storage in Deep Geologic Formations for Climate Change Mitigation, vol. 2: Geologic Storage of Carbon Dioxide with Monitoring and Verification, Elsevier Publishing, Oxford, UK, 2005, pp. 1143–1172.
[58] VROM, Interventiewaarden gevaarlijke stoffen 2007, Ministerie van Volkshuisvesting Ruimtelijke Ordening en Milieu, Den Haag, 2008.
[59] VROM, Circulaire 'Zonering langs hogedruk aardgas-transportleidingen', Ministerie van VROM, Den Haag, the Netherlands, 1984.
[60] P. Hopkins, R. Fletcher, R. Palmer-Jones, A method for the monitoring and management of pipeline risk—a simple pipeline risk audit (SPRA), in: 3rd Annual Conference on 'Advances in Pipeline Technologies & Rehabilitation '99', Abu Dhabi, 1999.
[61] I. Corder, The application of risk techniques to the design and operation of pipelines, in: IMechE Conference on 'Pressure Systems: Operation, and Risk Management', London, 1995.
[62] W.K. Muhlbauer, Enhanced Pipeline Risk Assessment. Part 1. Probability of Failure Assessments, WKM Consultancy, 2006.
[63] C. Vlek, Environmental versus individual risk taking: perception, decision, behaviour, in: Encyclopedia of Applied Psychology, Academic Press, San Diego, CA, 2004.
[64] VROM, Regeling externe veiligheid inrichtingen, 2009.
[65] J.C. Refsgaard, J.P. van der Sluijs, A.L. Højberg, P.A. Vanrolleghem, Uncertainty in the environmental modelling process—a framework and guidance, Environ. Modell. Softw. 22 (11) (2007) 1543–1556.
[66] A. Mazzoldi, T. Hill, J.J. Colls, CFD and Gaussian atmospheric dispersion models: a comparison within leakages from carbon dioxide transportation and storage facilities, Atmos. Environ. 42 (34) (2008) 8046–8054.
[67] HSE, The Health and Safety Risks and Regulatory Strategy Related to Energy Developments, Health and Safety Executive, London, 2006.